2Pa5-5

Comparison between Thermal Strain and Acoustic Radiation Force Imaging Methods for Estimation of Heat Source Distribution of High-Intensity Focused Ultrasound

HIFU加熱分布推定における熱ひずみイメージング法と音響放射力イメージング法の比較

Nozomi Obara[1‡], Shin-ichiro Umemura[1], and Shin Yoshizawa[2]
([1] Grad. School Biomed. Eng., Tohoku Univ.; [2] Grad. School Eng., Tohoku Univ.)
小原望 [1‡]，梅村晋一郎 [1]，吉澤晋 [2] ([1] 東北大院　医工, [2] 東北大院　工)

1. Introduction

High-intensity focused ultrasound (HIFU) is a non-invasive modality for cancer treatment. In this method, ultrasound generated outside a body is focused on a target tissue and induce thermal coagulation. From these principles, targeting the treatment region in advance is needed for treatment safety and efficacy, because the actual heating region can be shifted from the geometric focal point due to acoustic phenomena such as ultrasonic refraction, scattering, and tissue absorption.

Acoustic radiation force impulse (ARFI) imaging[1)] is a method which provides ARF by HIFU exposure and the estimation of the focal region from the displacement caused by ARF on the assumption that ultrasonic absorption is proportional to the attenuation. Another method is thermal strain (TS) imaging[2)] by which a small temperature rise is determined based on a linear relationship between strain and temperature rise by considering tissue expansion and local changes in sound speed.

In this study, both ARFI imaging and TS imaging were carried out and compared using the same chicken tissue.

2. Material and Method

2.1 Acoustic radiation force imaging

Focused ultrasound generates the acoustic radiation force F in a soft tissue expressed as,

$$|F| = \frac{2\alpha I}{c} \tag{1}$$

where α is the amplitude attenuation coefficient of the tissue, c is the sound speed of the tissue, and I is the acoustic intensity.

On the other hand, the heat Q generated by HIFU exposure is given by,

$$Q = 2\alpha_a I \tag{2}$$

where α_a is the amplitude absorption coefficient. The absorption coefficient is assumed to be proportional to the attenuation coefficient. Therefore, the distribution of heat caused by HIFU is proportional to the calculated displacement in the uniform tissue.

2.2 Thermal strain imaging

The temperature change generated by HIFU exposure results in a time-shift on the echo given by,

$$\delta t(z) = 2\int_0^z \left[\frac{1+\alpha(z')\delta\theta(z')}{c(z',\theta(z'))} - \frac{1}{c(z',\theta_0)} \right] dz' \tag{3}$$

where $\alpha(z')$ is the linear coefficient of thermal expansion, $\theta(z') = \theta_0 + \delta\theta(z')$ is the temperature in depth z', θ_0 is the initial temperature, and $c(z',\theta(z'))$ is the sound speed at depth z' and temperature $\theta(z')$. In the temperature range of interest, the sound speed $c(z,\theta(z))$ is expressed by,

$$c(z,\theta(z)) = c_0(z)(1+\beta(z)\delta\theta(\theta)) \tag{4}$$

where $c_0(z) = c(z,\theta_0)$, $\beta(z) = \frac{1}{c_0(z)} \cdot \left.\frac{\partial c(z,\theta)}{\partial\theta}\right|_{\theta=\theta_0}$.

Under condition of $|\beta(z)\delta\theta(z)| \ll 1$, temperature change in depth z is given by,

$$\delta\theta(z) = \frac{c_0(z)}{2}\left(\frac{1}{\alpha(z)-\beta(z)}\right) \cdot \frac{\partial}{\partial z}(\delta t(z)) \tag{5}$$

The term $\frac{1}{\alpha(z)-\beta(z)}$ depends on the property of tissue. Therefore, the distribution of temperature change is estimated by the strain of the echo signal in uniform tissue[2)].

2.3 Experimental setup and sequence

The experimental setup is shown in **Fig. 1**. A 256-ch HIFU transducer with both diameter and focal length of 120 mm was set at an acrylic tank filled with degassed water. The transducer was driven at 1 MHz by a staircase voltage driving system (Microsonic). In the central hole of the transducer, an imaging probe driven at a center frequency of 3.5 MHz was equipped. It connects to the imaging system (Verasonics) to acquire RF data.

nozomi.obara.p3@dc.tohoku.ac.jp

Through an experiment, a chicken breast having soaked in degassed saline is used as a sample tissue.

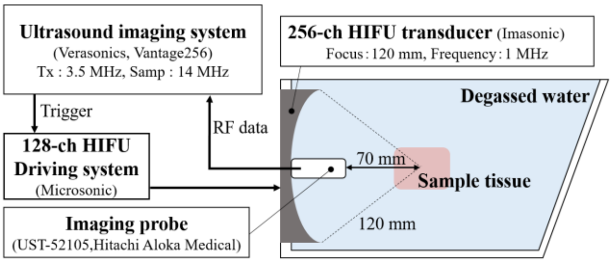

Fig. 1 Schematic of experimental setup

Fig. 2(a) shows the sequence of HIFU exposure and RF acquisition in ARFI imaging. The exposure duration and intensity of HIFU were 1 ms and 3 kW/cm^2, respectively. Before and after the HIFU exposure, RF data was acquired by a single plane wave transmission. To prevent an interference, the interval between HIFU exposure and RF data acquisition was set to 700 μs. **Fig. 2(b)** shows the sequence in TS imaging. The HIFU exposure duration were changed in a range of 0.05 s – 0.9 s and intensity kept constant at 924 W/cm^2. Before and after the HIFU exposure, RF data was acquired with 5 diverging waves steered at angles of -6, -3, 0, 3, and 6° . The interval between HIFU exposure and RF data acquisition were 0.05, 0.5, and 1 s, which ARF influence is thought to be non-existent. In both imaging methods, the axial displacement is calculated from the frames before and after the HIFU exposure by applying the autocorrelation method[3]. As for TS imaging, the axial displacement was differentiated with respect to the axial direction to obtain the strain.

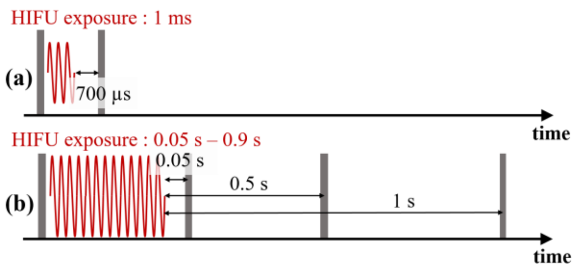

Fig. 2 Sequence of HIFU and RF acquisition
(a) ARFI imaging (b) TS imaging

3. Result and Discussion

Fig. 3 shows the calculated strain averaged in ROI (Axial: 67.2 mm to 69.6 mm, Lateral: -2.01 mm to -0.22 mm) as a function of HIFU duration. For a series of scatterings at each acquisition time, a linear relation between the strain and HIFU duration was obtained within the range of the measurement.

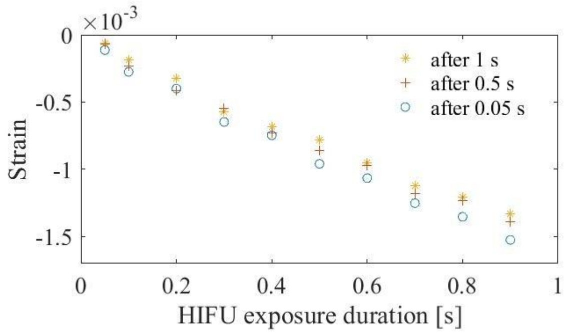

Fig. 3 The calculated strain averaged in ROI vs. HIFU exposure duration

Figs. 4(a) and **4(b)** show the distribution of displacement in ARFI imaging and that of strain in TS imaging (Duration: 0.9 s, Acquired after 1 s). The position of the peak value found in $z = 68$ mm was well agreed. The full widths half maximum (FWHM) of displacement and strain were 18.6 mm and 9.85 mm along the axial direction, respectively. In terms of lateral direction, the FWHM of displacement and strain were 5.91 mm and 3.46 mm, respectively. The result indicates that displacement estimated by ARFI imaging seems to be expanded due to the shear wave propagation.

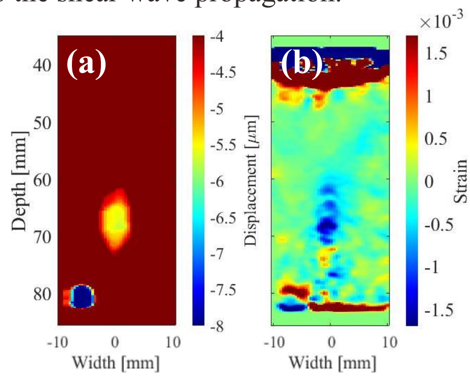

Fig. 4 (a) Displacement map in ARFI imaging
(b) Strain map in TS imaging

4. Conclusion

In this study, ARFI and TS imagings in the same chicken tissue were compared. The results imply the capability of quantitative calibration of temperature in TS imaging. In addition, the difference of the distribution depending upon the physical phenomenon between the two imaging methods was observed.

References

1. R.Iwasaki, et al.: Jpn. J. Appl. Phys. **56**, (2017) 07JF23.
2. S.Claudio, et al.: IEEE Trans. UFFC, **45**, (1998) 1088.
3. T.Shiina, et al.: J.Med.Ultrason. **29**, (2002)119.